Journal of Statistical Mechanics: Theory and Experiment
An IOP and SISSA journal

Néel and disordered phases of coupled Heisenberg chains with $S = \frac{1}{2}$ to $S = 4$

S Moukouri

Department of Physics and Michigan Center for Theoretical Physics, University of Michigan, 2477 Randall Laboratory, Ann Arbor, MI 48109, USA
E-mail: moukouri@umich.edu

Received 27 October 2005
Accepted 9 January 2006
Published 6 February 2006

Online at stacks.iop.org/JSTAT/2006/P02002
doi:10.1088/1742-5468/2006/02/P02002

Abstract. We use the two-step density-matrix renormalization group method to study the effects of frustration in Heisenberg models for $S = \frac{1}{2}$ to 4 in a two-dimensional anisotropic lattice. We find that as for $S = \frac{1}{2}$ studied previously, the system is made up of nearly disconnected chains at the maximally frustrated point, $J_{\rm d}/J_{\perp} = 0.5$, i.e., the transverse spin–spin correlations decay exponentially. This leads to the following consequences: (i) all half-integer spins systems are gapless, behaving like a sliding Luttinger liquid as for $S = \frac{1}{2}$; (ii) for integer spins, there is an intermediate disordered phase with a spin gap, with the width of the disordered state roughly proportional to the 1D Haldane gap.

Keywords: density matrix renormalization group calculations, quantum phase transitions (theory)

J. Stat. Mech. (2006) P02002

Contents

1. Introduction

An important theorem of Dyson, Lieb and Simon (DLS) states that the Heisenberg Hamiltonian on bipartite lattices with $S \geq 1$ has long range order in the ground state [1, 2]. We now know from quantum Monte Carlo simulations [3] that this result extends to $S = \frac{1}{2}$ systems. There is current interest in how a disordered state emerges out of the Néel state. This question is important to the physics of frustrated materials where some systems exhibit no magnetic order down to the experimentally accessible temperatures and are thus believed to be disordered in the ground state. A disordered phase may also be relevant in the theory of high-temperature superconductors. This issue and the related one of the eventual role of Berry phases was hotly debated in the late 1980s and early 1990s soon after the discovery of the high-T_C materials [4]–[8]. Many possible disordered states were proposed but none of them gained consensus. For an extensive discussion on this topic, we refer the reader to the book by Fradkin [23].

In the search for the nature of a ground state of a quantum Hamiltonian, there is another useful theorem given by Lieb, Schultz and Mattis (LSM) [20], initially formulated for 1D systems and later extended to 2D systems by Affleck [8], which restricts the

J. Stat. Mech. (2006) P02002

possible ground states of half-integer spin systems: either the ground state is degenerate (presumably due to a broken symmetry) or it is unique and gapless without any long range order. For Heisenberg Hamiltonians, the latter possibility appears difficult to realize in 2D because dimer–dimer or spin–spin correlations have a power law decay in 1D. It would thus be expected that interchain couplings will lead to long range order in one of the two channels. If the magnetic order is frustrated, a dimerization would be expected. Frustrated spin models often involve competitions between two magnetic orders; the expected dimerized phase is believed to lie between these magnetic phases. A possible alternative to this scenario allowed by the LSM theorem is the occurrence of a disordered gapless state at the transition between the magnetic phases.

In recent publications [24, 25], we have studied the possible emergence of a disordered state in a model of coupled Heisenberg chains. This model is a spatially anisotropic version of the well studied J_1–J_2 model. The model essentially retains the physics of the J_1–J_2 model: it presents a phase transition between two magnetic phases. The first phase is a Néel phase characterized by the ordering wavevector $K = (\pi, \pi)$. The order parameter in this phase is maximal in the absence of the diagonal coupling J_d. It decreases as J_d is increased until it vanishes at the maximally frustrated point. Beyond this point, another Néel state with $K = (\pi, 0)$ becomes the ground state. The existence of these two phases was predicted in numerous studies [17] of the isotropic ($J_\perp = 1$) version of this model. But what has caused the continuing interest in this simple model is the question of whether there is an intermediate phase between these two magnetic phases. Simple physical arguments suggest the existence of such a phase because the two states are associated with subgroups of the $SU(2)$ symmetry group of the spin Hamiltonian and of the C_4 symmetry group of the square lattice that do not include each other. From the Landau theory we know that a continuous transition from these two phases is forbidden. Initial suggestions for the possible intermediate phase were the resonating valence bond (RVB) [36] phase, flux phases [32, 35], chiral spin liquid [34] and the spin–Peierls (SP) phase [21]. The SP phase has lately emerged as the front runner. It causes the same type of difficulty as the direct transition between two magnetic phases, since in that case the transition is between a magnetic state that breaks the spin rotational symmetry but not the lattice translational symmetry and a dimerized state that breaks the lattice translational symmetry but not the spin rotational symmetry. The transition to the SP phase has triggered an interesting proposal of an extension of the conventional Landau–Ginzburg–Wilson (LGW) theory of second-order phase transitions [37].

It seems, however, that this theory does not apply to the J_1–J_2 model, where we did not find any evidence of an intermediate phase for $S = \frac{1}{2}$. Numerical data suggests a transition, which seems to be of second order, between the two magnetic phases at the maximally frustrated point for both the anisotropic and isotropic models [22]. At the transition point, the competing magnetic orders neutralize each other and the system behaves like a collection of loosely bound chains, even if the bare interactions are not small. Classically, the ground state is degenerate at this point. This degeneracy is lifted by quantum fluctuations. In [22, 25], we have shown that among all the possible clusters, chains offer the best compromise between minimizing the energy and avoiding frustration, at the same time. At the maximally frustrated point, the transverse interactions seem to be irrelevant, i.e., up to the largest lattice size studied, transverse spin–spin correlations decay exponentially and the longitudinal correlations revert to those of decoupled chains.

J. Stat. Mech. (2006) P02002

This disordered state is a singlet and gapless, consistent with the LSM theorem [8, 20]. It is reminiscent of a sliding Luttinger liquid (SLL) found in models of coupled fermion chains [9]–[11]. It thus appears that the intermediate region where a disordered phase has long been thought to exist is just a critical region. That is why it has resisted various approaches for nearly two decades. At the maximally frustrated point, the correlation functions are 1D-like; thus the rotational spin symmetry of the system is restored. In fact such a transition between these two magnetic phases already exists in the unfrustrated model when the transverse exchange parameter, $J_\perp$, is varied from positive values to negative values. At the point $J_\perp = 0$, there is a transition from 2D to 1D, where properties are identical to that of the maximally frustrated point. The only difference between the case $J_\perp = 0$ and the maximally frustrated point is the presence of irrelevant transverse terms which do not change the long distance behaviour of the correlation functions as shown in [25]. From this result the LGW theory applies if it is assumed that the system's group of symmetry at the critical point contains the groups of symmetry of the two magnetic phases.

It is important to study how this interesting physics extends to larger spin systems, first, because many frustrated systems contain larger spins and, second, because there are some interesting predictions from large S approaches about the emergence of a disordered phase from a Néel phase as a function of S. Affleck [8] argued that since the LSM theorem does not apply to integer spin systems, there might be a distinction between integer and half-integer spin systems in 2D as well. Haldane [7] discussed the notion that in addition to the now well established difference in behaviour between half-integer and integer spins in one dimension [19], there might be a difference between odd and even integer spins in two dimensions due to the effects of the Berry phase. Read and Sachdev carried out a large N analysis of the possible disordered phase as a function of the value of the large N equivalent of the spin. Their results were consistent with Haldane's predictions. Three types of disordered state were predicted. For half-integer spins, the non-magnetic phase is a SP phase which breaks the translational symmetry along the two directions of the square lattice. For odd integer spins, the non-magnetic state is made of weakly coupled chains, i.e., the translational symmetry is broken along one direction only. Finally for even integer spins, the disordered state is the valence bond solid, like the Affleck–Kennedy–Lieb–Tasaki (AKLT) state [33], i.e., it does not break any translational symmetry.

In the large S approaches the Heisenberg model is mapped onto the non-linear sigma model (NLσ) with a Berry phase term. This mapping is only approximate [19, 30] and there can be some subtle differences from the original model [30]. Indeed, the realization of the Haldane conjecture in 1D shows their power. But, in the absence of exact results for small S, it is impossible to know whether their predictions of a disordered phase extend to small S. Another potential problem is that the mapping to the σ model assumes the presence of a smooth configuration of spins. This is true in the weak coupling regime (Néel ordered phase), but this assumption may break down in the strong coupling regime (disordered phase). In one dimension, the σ model coupling constant is given by $g = 2/(\sqrt{S(S+1)}\sqrt{1-4J_2})$ [30]. Thus for $S = \frac{1}{2}$, the equivalence of the two models breaks down at $J_2 = 0.25$, i.e., close to the transition to a dimerized state. Such a breakdown seems to occur in the J_1–J_2 model where, as seen above, the large N predictions conflict for $S = \frac{1}{2}$ with the TSDMRG in the J_1–J_2 model. But since spin half-integer systems are critical, it could be objected that the behaviours seen in our numerical

studies are due to finite size effects. For large enough lattices there might be a relevant interaction which can drive the system to a SP phase as predicted for large N. Though this scenario appears to be unlikely, as discussed in [22], it cannot be completely rejected. In principle, one would expect a different behaviour for integer spin systems which are known to have a spin gap in 1D [19].

In this paper, we applied the TSDMRG to study $S = \frac{1}{2}, 1, \frac{3}{2}, \ldots, 4$ systems in the anisotropic 2D Hamiltonian (1). Our results in the absence of frustration are in agreement with the DLS theorem [1, 2]. We find that for all S the ground state is ordered in the absence of frustration. For all S except for $S = \frac{1}{2}$, the order parameter is large enough that the extrapolated values are reliable. This result constitutes a non-trivial test of the TSDMRG, since the TSDMRG starts from decoupled chains which are disordered. When the frustration is turned on, the general mechanism found for the destruction of the Néel phase is the severing of the frustrated bonds in the transverse direction, leading to a disordered state with the transverse correlations that decay exponentially at the critical point as previously found for $S = \frac{1}{2}$. However, a different conclusion is to be drawn for half-integer S and for integer S for which the LSM theorem does not apply. All half-integer systems are similar to $S = \frac{1}{2}$. The disordered state is confined at the critical point; it has a SLL character. But for integer S, because of the Haldane gap Δ_{H} in the chain, there is an intermediate phase whose width is roughly $\propto \Delta_{\mathrm{H}}$.

This paper is organized as follows. In the next section we discuss the model and the method. In section 3, we present extensive results for $S = 1$ systems. This analysis is similar to the one made for spin $\frac{1}{2}$ systems in [22]. In section 4 the results for systems with $S = \frac{1}{2}$ to 4 are presented. In section 5, we present our conclusions.

2. Model and method

2.1. Model

We apply the TSDMRG [24, 25] to the spatially anisotropic Heisenberg Hamiltonian

$$H = J_{\parallel} \sum_{i,l} \mathbf{S}_{i,l}\mathbf{S}_{i+1,l} + J_{\perp} \sum_{i,l} \mathbf{S}_{i,l}\mathbf{S}_{i,l+1} + J_{\mathrm{d}} \sum_{i,l} (\mathbf{S}_{i,l}\mathbf{S}_{i+1,l+1} + \mathbf{S}_{i+1,l}\mathbf{S}_{i,l+1}) \tag{1}$$

where $J_{\parallel}$ is the intra-chain exchange parameter and is set to 1; $J_{\perp}$ and J_{d} are respectively the transverse and diagonal interchain exchanges. This model is the object of current interest [12, 13, 18, 25]. It is a starting point for understanding the J_1–J_2 model which is recovered when $J_{\parallel} = J_{\perp} = J_1$ and $J_{\mathrm{d}} = J_2$. It retains the basic physics of the J_1–J_2 model and has the advantage that in the limit $J_{\perp}, J_{\mathrm{d}} \ll 1$, well tested 1D results can be used to initialize a perturbative RG analysis.

2.2. The two-step DMRG

In the TSDMRG, to study a 2D lattice of size $L \times (L+1)$ (we will refer to the 2D systems only by their linear dimension L), we start by applying the usual 1D DMRG (m_1 states are kept) or exact diagonalization (ED) to a single chain l of length L to obtain m_2 low lying eigenstates and eigenvalues, ϕ_{n_l}, ϵ_{n_l}, $n_l = 1, 2, \ldots, m_2$, respectively. Then, we formally write the tensor product of the eigenstates of the $L+1$ chains,

$$\Phi_{[n]} = \phi_{n_1}\phi_{n_2}\cdots\phi_{n_{L+1}}. \tag{2}$$

J. Stat. Mech. (2006) P02002

$\Phi_{[n]}$ is an eigenstate of the Hamiltonian with $J_\perp = 0$ and $J_\mathrm{d} = 0$, $[n] = (n_1, n_2, \ldots, n_{L+1})$. The $\Phi_{[n]}$ constitute a many-body basis of the truncated Hilbert space of the tensor product of $L+1$ chains. The corresponding eigenvalue is

$$E_{[n]} = \epsilon_{n_1} + \epsilon_{n_2} + \cdots + \epsilon_{n_{L+1}}. \tag{3}$$

The 2D Hamiltonian (1) is then projected onto this truncated basis to yield an effective one-dimensional Hamiltonian which is studied using the DMRG.

The TSDMRG is perturbative; but the expansion is made in the smaller term of the Hamiltonian itself not the Green's function or the ground state wavefunction. We have shown that starting from a disordered state, the TSDMRG is able to reach the ordered state without any addition of a term that explicitly breaks the symmetry such as a magnetic field. The TSDMRG was tested against the quantum Monte Carlo method (QMC) in [25] and against ED in [27]. The TSDMRG is variational; its performance can be systematically improved by increasing m_1 and m_2. Key indicators of the performance of the TSDMRG are the truncation error ρ_1 during the first step, the width δE of the m_2 states kept and the truncation error ρ_2 during the second step. In principle, it is necessary that the ratio of δE over the transverse coupling be large for the TSDMRG to yield great accuracy. Typically, one must have $\delta E/J_\perp \approx 10$. If this condition is fulfilled and the m_2 states are accurate enough, i.e., ρ_1 is small, the TSDMRG method can reach QMC accuracy. So far, this has been achieved only for small couplings $J_\perp \lesssim 0.1$ and lattice sizes of up to $L = 16$ keeping up to $m_2 = 96$. The amount of calculation involved remains modest and so far it has been done on a workstation. The accuracy decreases by increasing $J_\perp$ leading to less accurate results in the ordered state. But when both $J_\perp$ and J_d are turned on, the performance of the TSDMRG becomes more complex as we will see below.

In this work, the calculations for $S = 1$ were performed similarly to those for spin $S = \frac{1}{2}$ systems in [22]. In most cases, ED was applied during the first step. In some cases, i.e., some runs of $L = 10$ and all runs of $L = 12$, a single DMRG iteration was used. For instance for $L = 10$ and $S = 1$, when $m_1 = 81$ states are kept, a single DMRG iteration is necessary to reach the desired size. For this calculation, we kept up to $m_2 = 96$ states during the second TSDMRG step. For the maximum performance of the algorithm, it is necessary that $J_\perp$ be of the order of the finite size gap of the single chain Δ_L. For $S = 1$, $\Delta_L \to \Delta_\mathrm{H}$ when $L \to \infty$, where $\Delta_\mathrm{H} = 0.4107$ [16] is the Haldane gap. A second condition to fulfil is $\delta_L \gg J_\perp$ where δ_L is the width of the retained eigenvalues. As noticed in [22], the TSDMRG is more accurate in the highly frustrated regime. In figure 1 we show the truncation error, ρ_2, when two states are targeted in the second step as a function of J_d for $S = 1$ and $J_\perp = 0.4$. ρ_2 is minimal near $J_\mathrm{d} = 0.22$. At this point the system is an assembly of nearly disconnected chains; the DMRG is thus expected to perform better.

2.3. Illustration in the $S = 1$ case

We now wish to provide a detailed description of a typical TSDMRG calculation. For this illustration, $S = 1$ and $L = 12$, i.e., following the convention set above, the size of the 2D lattice is 12×13. We start the usual 1D DMRG iteration keeping $m_1 = 243$ states, i.e., the initial superblock size is $L = 12$. At this point the DMRG is equivalent to ED. At the next iteration, the superblock size is $L = 14$; its total number of states is $M_\mathrm{s} = (3 \times 243)^2$. The size of the reduced superblock (the superblock minus the two

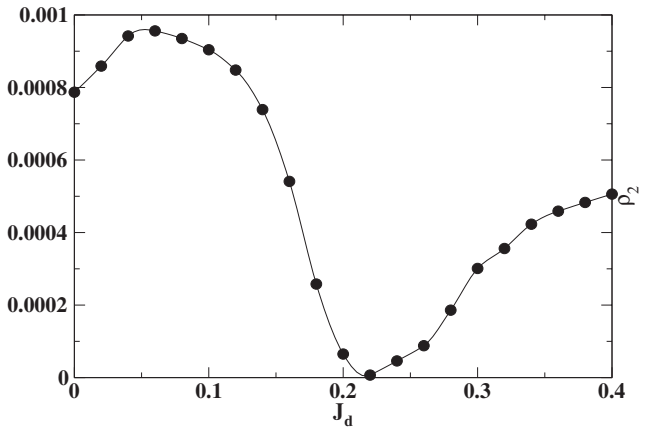

Figure 1. Truncation error in the second TSDMRG step as function of $J_{\rm d}$ for $J_\perp = 0.4$, $S = 1$ and $L = 10$; ED was performed in the first step and in the second step; $m_2 = 64$.

single-site blocks) is $L = 12$. During this iteration, spins sectors with $S^z_T = 0, \pm1, \pm2, \pm3$ are targeted. The lowest states in each of these sectors for $L = 12$ have respectively the following energies: $E_0 = -16.8696$, $E_{\pm1} = -16.3854$, $E_{\pm2} = -15.5294$, $E_{\pm3} = -14.2778$. The truncation error is 7.3×10^{-7}. The reduced superblock is then diagonalized and the $m_2 = 64$ lowest lying states are kept. The energy of the highest state among these m_2 states is -14.2687 which is lower than $E_{\pm4} = -12.6524$, the lowest states of the $S^z_T = \pm4$ sectors. For this reason, these sectors were not targeted. The operators $\mathbf{S}_i$ at each site are stored and updated.

From the energy levels above, we see that the finite size spin gap is $\Delta_L = 0.4842$, which is not very far from its value $\Delta_{\rm H} = 0.4107$ in the thermodynamic limit. Our choice of $J_\perp = 0.4$ ensures that the chains will effectively be coupled at this size. The matrix O whose columns are made of the m_2 vectors ϕ_n kept is used to express all the operators in the truncated reduced superblock basis,

$$\bar{\mathbf{S}}_i = O^\dagger \mathbf{S}_i \delta_{3,3'} O; \tag{4}$$

the intra-chain Hamiltonian is likewise updated:

$$h = O^\dagger (h_{\rm B_1} \delta_{3,3'} + h_{\rm B_3} \delta_{1,1'}) O. \tag{5}$$

In these equations, we have adopted the usual convention that the different blocks of the superblock are labelled 1–2–3–4. For PBC, blocks 2 and 4 are made of a single site and blocks 1 and 3 are the largest blocks. In equation (4), it is supposed that the spin to update is in block 1. In equation (5), $h_{\rm B_i}$ represents the internal Hamiltonian of block i. The first step ends with the updating of these operators.

Each chain may now be viewed as a super 'spin' with additional internal degrees of freedom due to the different sites. A chain l is described by its 'spin' value $\tilde{\mathbf{S}}_l = (\bar{\mathbf{S}}_{il}, i = 1, \ldots, L)$ and its internal Hamiltonian h_l. h_l is diagonal in the basis of the m_2 states kept. The effective first-order Hamiltonian which approximates the original 2D Hamiltonian is now given by

$$H_{\rm eff} = \sum_l h_l + J_\perp \sum_l \tilde{\mathbf{S}}_l * \tilde{\mathbf{S}}_{l+1} + J_{\rm d} \sum_l \tilde{\mathbf{S}}_l \times \tilde{\mathbf{S}}_{l+1}, \tag{6}$$

where

$$\tilde{\mathbf{S}}_l * \tilde{\mathbf{S}}_{l+1} = \sum_i \bar{\mathbf{S}}_{i,l}\bar{\mathbf{S}}_{i,l+1} \tag{7}$$

and

$$\tilde{\mathbf{S}}_l \times \tilde{\mathbf{S}}_{l+1} = \sum_i \bar{\mathbf{S}}_{i,l}\bar{\mathbf{S}}_{i+1,l+1} + \bar{\mathbf{S}}_{i+1,l}\bar{\mathbf{S}}_{i,l+1}. \tag{8}$$

We then proceed to compute the low lying states of H_{eff} using the conventional DMRG again. For this simulation we keep m_2 states and use 3 blocks instead 4 to form the superblock.

As expected from the study of $S = \frac{1}{2}$ systems, the TSDMRG is more accurate in the highly frustrated regime than in the unfrustrated case. ρ_2 is relatively large in the unfrustrated regime because of the relatively large value of the interchain coupling. The same simulation with $J_\perp = 0.2$ leads to an improvement of factor 10. It is worth noting that the superblock size in this step is m_2^3. We are able to reach $m_2 = 100$ on a workstation; this remains modest with respect to what can be achieved on today's supercomputers. For the multi-chain DMRG superblock sizes of about 100 times larger are accessible [14]; this means that it is possible to reach $m_2 \approx 500$ on a supercomputer. This would increase the current accuracy of the TSDMRG by two or more orders of magnitude. This shows the great potential of the TSDMRG. These possibilities are under exploration.

Since the TSDMRG is variational, we expect it to underestimate physical quantities. A key quantity which measures the accuracy of the TSDMRG besides ρ_1 and ρ_2 is the transverse correlation function,

$$C_l = \langle S_{L/2,L/2+1} S_{L/2,L/2+l} \rangle. \tag{9}$$

For fixed (m_1, m_2), the magnitude of C_l is underestimated by the TSDMRG. This was seen in the study of $S = \frac{1}{2}$ in [25] where the TSDMRG was compared to QMC approaches. We may expect that if m_1 is large enough that the states needed to compute the transverse matrix elements are computed accurately, C_l will only depend on m_2. This is seen in figure 2, where C_l is nearly independent of m_1. In that case, as shown in figure 3, the magnitude of C_l will increase with m_2 as we would expect from the variational nature of the TSDMRG. We find that this is observed when both ρ_1 and ρ_2 are small enough, i.e., less than about 5×10^{-4}.

But deep in the magnetic regime, while the magnitude of C_l still increases with m_2 for a fixed m_1 as shown in figure 4, the m_1 dependence of C_l (not shown) is not completely clear. For a fixed $m_2 = 64$, the magnitude of C_l first decreases with increasing m_1 and then increases. The maximum variation of C_l from $m_1 = 81$ to 243 is less than 0.02. Given that $\rho_2 \approx 10^{-3}$ in this region, we are clearly at the limit of the TSDMRG for the values of m_1 and m_2 used in this simulation. This limit is the illustration of the well known slow convergence of the DMRG for gapless systems.

3. Results for $S = 1$

The case of spin $\frac{1}{2}$ has been extensively studied in [22, 25]. We were able to reach lattice sizes of up to 64×65 and show that as seen in QMC simulations, the system is ordered in the absence of frustration for small $J_\perp$. But when $J_\text{d} \neq 0$, we have shown that in the

J. Stat. Mech. (2006) P02002

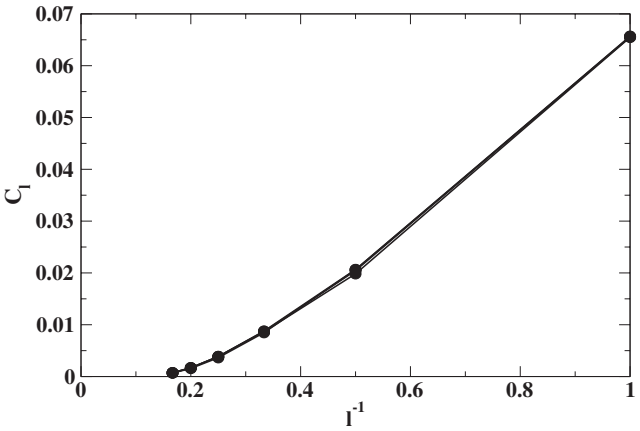

Figure 2. Transverse spin–spin correlation as a function of distance and $m_1 = 81$, 108, 162, 243 (bottom to top) for $m_2 = 64$ at $J_\perp = 0.4$, $J_\mathrm{d} = 0.2$, $S = 1$ and $L = 12$.

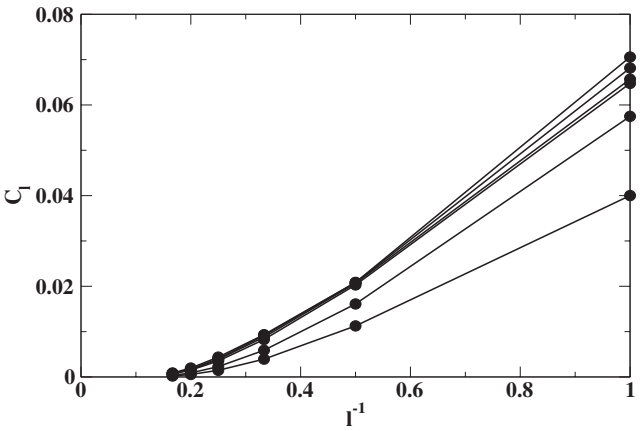

Figure 3. Transverse spin–spin correlation as a function of distance and $m_2 = 16$, 32, 64, 80, 96 (bottom to top) for $m_1 = 162$ at $J_\perp = 0.4$, $J_\mathrm{d} = 0.2$, $S = 1$ and $L = 12$.

vicinity of $J_\mathrm{d}/J_\perp \approx 0.5$ the system is made of weakly coupled chains even when $J_\perp$ and J_d are not small. This finding of the TSDMRG was checked using ED on small systems [27]. More careful simulations at the vicinity of the point $J_\mathrm{d}/J_\perp = 0.5$ revealed that the first-neighbour interchain correlation, i.e. the transverse bond strength, is equal to zero at the maximally frustrated point. The non-zero correlations, starting from the second neighbour, decay exponentially. These results lead us to conclude that the maximally frustrated point is a quantum critical point (QCP) between the two magnetic states (the second magnetic state is stable when $J_\mathrm{d} > 0.5J_\perp$). A possible argument against this conclusion is that at the maximally frustrated point, the system could be unstable against higher order terms such as a ring exchange term [13]. In the case of a two-leg ladder this term seems to lead to a dimerized state. There are however some strong indications that the dimerized state does not exist in this model as discussed in [22]. The mechanism for avoiding frustration is dividing the system into chains in which the frustrated bonds are

J. Stat. Mech. (2006) P02002

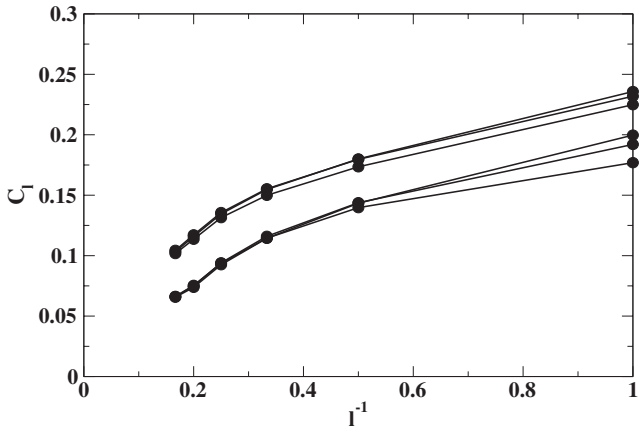

Figure 4. Transverse spin–spin correlation as a function of distance and $m_2 = 16$, 32, 64, 80, 96 (bottom to top) for $m_1 = 162$ at $J_\perp = 0.4$, $J_\mathrm{d} = 0$, $S = 1$ and $L = 12$.

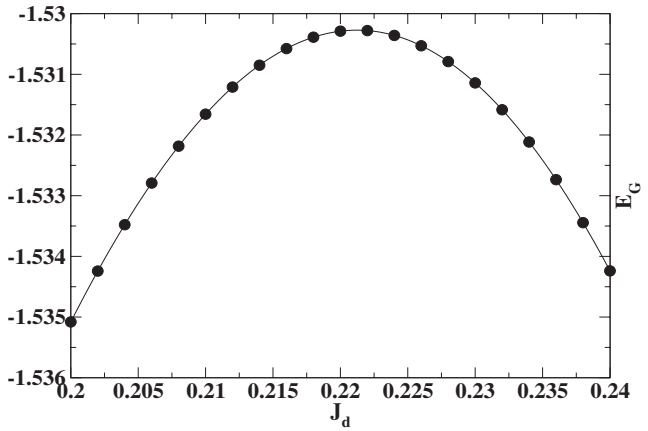

Figure 5. Ground state energy per site as a function of J_d for $J_\perp = 0.4$, $S = 1$ and $L = 12$.

severed. We will now study the extension of this mechanism to $S = 1$. We perform the same analysis as for $S = \frac{1}{2}$ for $L = 6$, 8, 10 and 12. For the first three values of L, ED is performed to obtain the m_2 lowest eigenvalues and the corresponding eigenstates of the chain. For $L = 12$ the DMRG was used; we kept $m_1 = 243$ states, i.e., one DMRG iteration was done from the $L = 10$ exact result. The truncation error was about 7×10^{-7}. The truncation error is relatively large because we used periodic boundary conditions. These m_2 low lying states were then used to generate the 2D lattices, i.e., 6×7, 8×9, 10×11 and 12×13 respectively.

3.1. Ground state energies

The curve of $E_\mathrm{G}(J_\mathrm{d})$ for $S = 1$, shown in figure 5, is similar to that of $S = \frac{1}{2}$. Starting from $J_\mathrm{d} = 0$, E_G increases until it reaches a maximum at $J_\mathrm{d}^{\max}$. It then decreases when J_d is further increased. The position of the maximum depends slightly on L and seems to

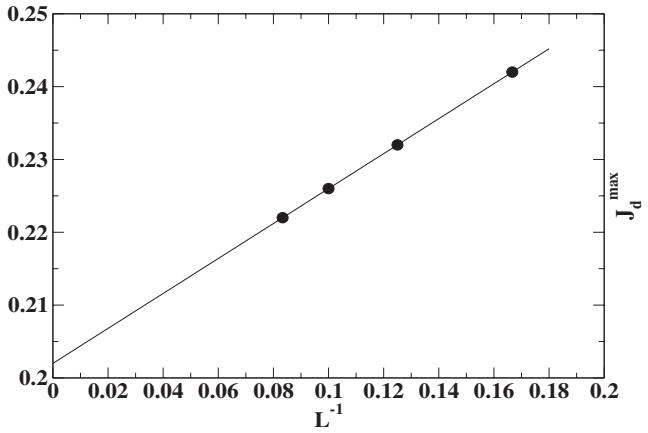

Figure 6. Maxima of the ground state energy as a function of L for $J_\perp = 0.4$, $S = 1$.

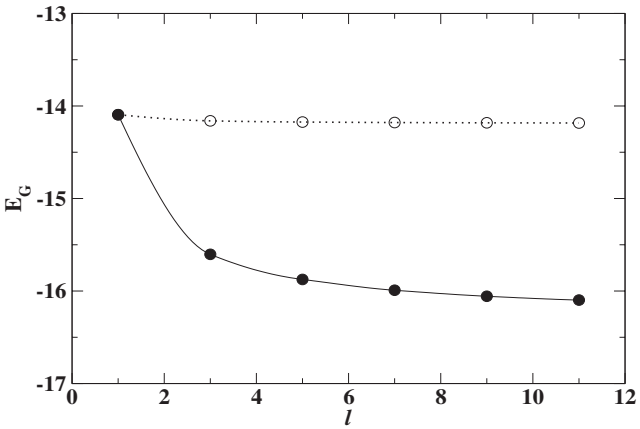

Figure 7. Ground state energy per chain as a function of the chain number for $J_\perp = 0.4$, $S = 1$, $L = 10$ for $J_\mathrm{d} = 0$ (filled circles) and $J_\mathrm{d} = J_\mathrm{d}^{\max}$ (open circles).

converge to $0.5J_\perp$ in the thermodynamic limit. $E_\mathrm{G}(J_\mathrm{d}^{\max})$ is very close to 1.53, the energy of decoupled chains, but always remains slightly lower. Thus as for $S = \frac{1}{2}$ the chains are very weakly bound, even though the bare interactions ($J_\perp = 0.4$ and $J_\mathrm{d} = 0.22$) are not small. $J_\mathrm{d}^{\max}$ depends on L as shown in figure 6 and, as in the case of $S = \frac{1}{2}$, it extrapolates to $0.5J_\perp$ in the thermodynamic limit.

$E_\mathrm{G}(l)$ shown in figure 7, where l is the number of chains, differs dramatically between when J_d is far from and close to $J_\mathrm{d}^{\max}$. Far from $J_\mathrm{d}^{\max}$, one of the two magnetic phases is highly favoured. Starting from an isolated chain, magnetic energy can be gained by increasing l, leading to the ordered state. The situation is different when $J_\mathrm{d} = J_\mathrm{d}^{\max}$; neither of the magnetic states is favoured. At this point, magnetic energy cannot be gained and $E_\mathrm{G}(l)$ is nearly independent of l; the system remains disordered as we will see below from the analysis of the correlation functions.

J. Stat. Mech. (2006) P02002

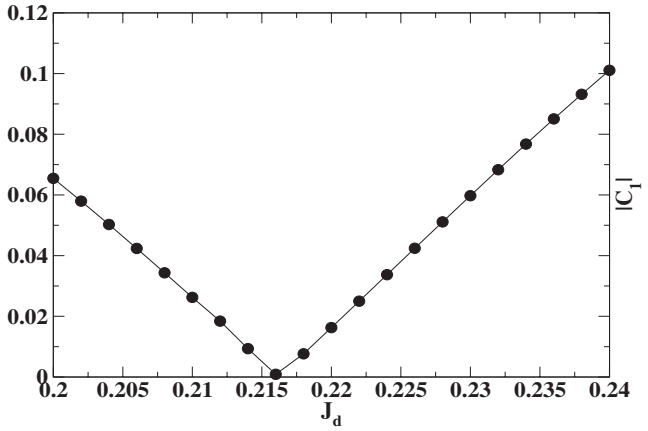

Figure 8. First-neighbour spin–spin correlation as a function of J_d for $J_\perp = 0.4$, $S = 1$, $L = 12$.

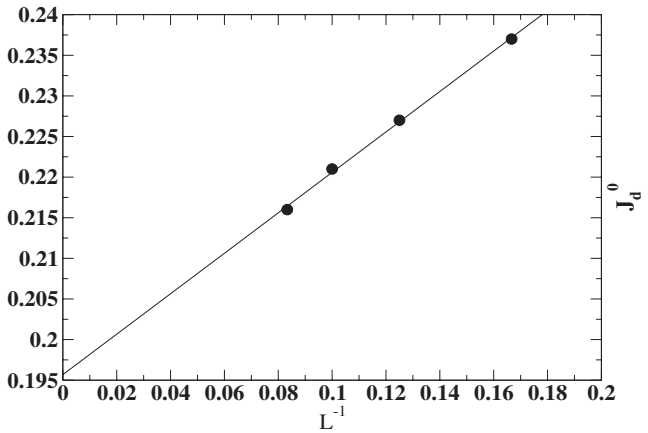

Figure 9. Minima of the first-neighbour spin–spin correlation as a function of L for $J_\perp = 0.4$, $S = 1$.

3.2. First-neighbour correlation

The transverse first-neighbour spin–spin correlation taken in the middle of the lattice

$$C_1 = \langle S_{L/2,L/2+1} S_{L/2,L/2+2} \rangle, \tag{10}$$

shown in figure 8, is also reminiscent of the $S = \frac{1}{2}$ case. C_1 vanishes linearly at $J_\mathrm{d} = J_\mathrm{d}^0$. J_d^0 is slightly different from $J_\mathrm{d}^{\max}$. This small difference is due to numerical error; this conclusion is supported by the more accurate results obtained for small $S = \frac{1}{2}$ systems in [22] where J_d^0 and $J_\mathrm{d}^{\max}$ are equal. The extrapolated J_d^0 (figure 9) as $L \to \infty$ is also in the vicinity of $0.5 J_\perp$.

3.3. Long distance correlations

The transverse spin–spin correlation function,

$$C_l = \langle S_{L/2,L/2+1} S_{L/2,L/2+l} \rangle, \tag{11}$$

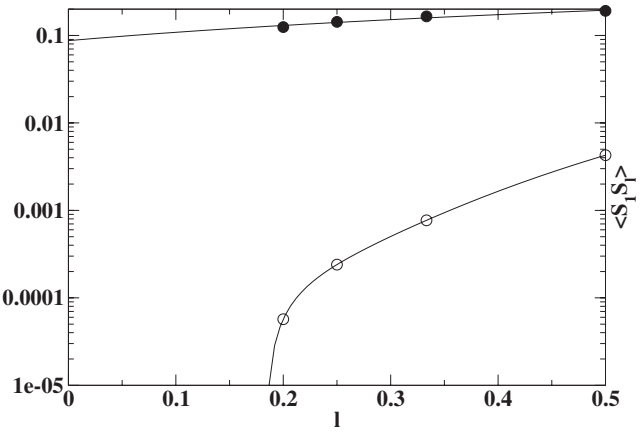

Figure 10. Transverse spin–spin correlation as a function of the distance for $L = 10$, $S = 1$, $J_\perp = 0.4$, $J_\mathrm{d} = 0$ (filled circles) and $J_\mathrm{d} = J_\mathrm{d}^{\max}$ (open circles).

is shown in figure 10 for an $L = 10$ system and $J_\perp = 0.4$. When $J_\mathrm{d} = 0$, C_l extrapolates to a finite value in the thermodynamic limit. This result is important because it shows the non-perturbative nature of the TSDMRG. Starting from an isolated chain which is disordered, the TSDMRG can reach the ordered phase. The ordered phase can be easily reached for spin larger than $S = \frac{1}{2}$ where quantum fluctuations are more important. The extrapolation of C_l for $S = \frac{1}{2}$ leads to a small negative value, as shown in figure 23 below. In this case, the order parameter is too small to be obtained from an extrapolation from relatively small systems; it is necessary to go to larger systems such as those studied in [25] in order to extrapolate to the correct thermodynamic limit. The extrapolated value of C_l does not however lead to the correct value of the magnetization since it is obtained from a system with a fixed L. A better estimation is given by the finite size analysis of the end-to-centre spin–spin correlation

$$C_L = \langle S_{L/2,L/2+1} S_{L/2,L+1} \rangle \tag{12}$$

shown in figure 11. C_L for $L \to \infty$ is roughly 0.06, again consistent with the existence of the long range order.

In the vicinity of $J_\mathrm{d}^{\max}$, C_l decays exponentially as seen in figure 10. For $l = 5$, his value is already four orders of magnitude smaller than in the case $J_\mathrm{d} = 0$. This is consistent with the nearly disconnected chain behaviour observed for E_G at this point.

3.4. Spin gaps

The variations of the spin gap Δ with l (for a fixed L), L and J_d are also consistent with the above findings. $\Delta(J_\mathrm{d})$ for $L = 10$ system is shown in figure 12. $\Delta(J_\mathrm{d} = 0)$ is about 0.05 (in this regime the gap is zero in the thermodynamic limit as we will see below); Δ remains relatively flat as J_d is increased until it reaches the vicinity of $J_\mathrm{d}^{\max}$. Near $J_\mathrm{d}^{\max}$, $\Delta(J_\mathrm{d})$ first sharply increases and reaches the finite size gap of an isolated chain. As $J_\mathrm{d} > J_\mathrm{d}^{\max}$, $\Delta(J_\mathrm{d})$ first sharply decreases and then becomes nearly constant at about 0.05. $\Delta(l)$ (figure 13) is reminiscent of $E_\mathrm{G}(l)$; in the unfrustrated case, the chains are effectively coupled. $\Delta(l)$ rapidly decreases from about 0.53 to 0.05 as l is varied from 1 to 11. At $J_\mathrm{d} = J_\mathrm{d}^{\max}$ however, $\Delta(l)$ is nearly independent of l.

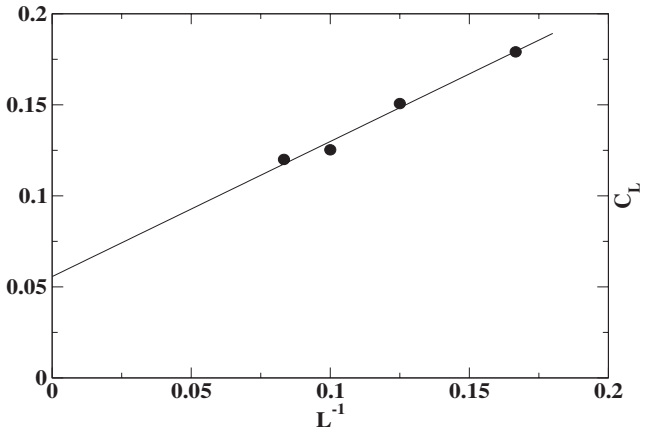

Figure 11. Centre-to-end spin–spin correlation as a function of L for $S = 1$, $J_\perp = 0.4$ and $J_\mathrm{d} = 0$.

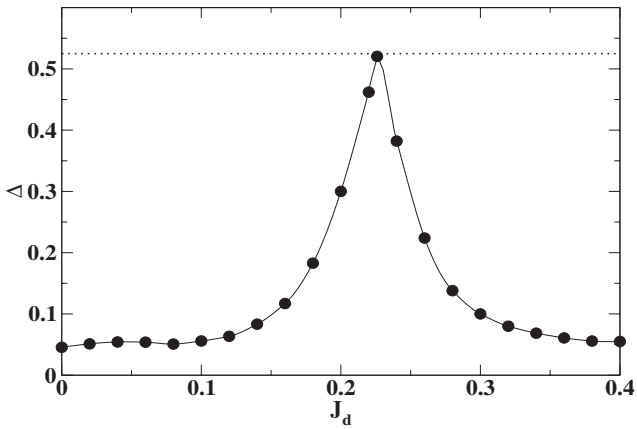

Figure 12. Gap as a function of J_d for $L = 10$, $S = 1$; the dotted line represents the single-chain gap.

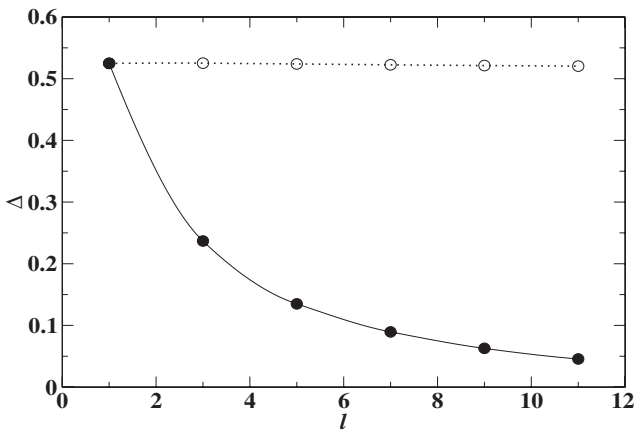

Figure 13. Gap as a function of the number of chains for $L = 10$, $S = 1$, $J_\perp = 0.4$, $J_\mathrm{d} = 0$ (filled circles) and $J_\mathrm{d} = J_\mathrm{d}^{\max}$ (open circles).

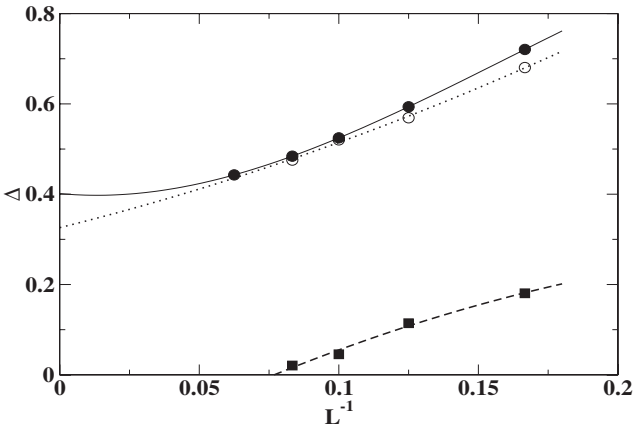

Figure 14. Gap as a function of L for $S = 1$, $J_\perp = 0$ and $J_\mathrm{d} = 0$ (single chain, filled circles), $J_\perp = 0.4$, $J_\mathrm{d} = 0$ (filled squares) and $J_\mathrm{d} = J_\mathrm{d}^{\max}$ (open circles).

The analysis C_L shows that for $J_\mathrm{d} = 0$, the system is ordered. We thus expect to have $\Delta(L) \to 0$ as $L \to \infty$. This is seen in figure 14 where $\Delta(L)$ is shown for $L = 6, 8, 10$ and 12 systems. The decay is faster than $1/L$; the extrapolation leads to a negative value. At $J_\mathrm{d} = J_\mathrm{d}^{\max}$ on the other hand, $\Delta(L)$ remains close to that of an isolated chain in all cases. The two functions are finite in the thermodynamic limit. This result shows the dramatic difference between $S = \frac{1}{2}$ and $S = 1$ systems. For $S = \frac{1}{2}$, an equivalent plot leads to a zero gap [22] at the maximally frustrated point. The extrapolated value for $J_\mathrm{d} = 0$, $\Delta = 0.4015$ agrees well with the current best estimate of the Haldane gap $\Delta_\mathrm{H} = 0.4107$. The difference is due to the relatively short chains, up to $L = 16$, that were used for the extrapolation, not to the DMRG that yielded highly accurate results for each size studied. Noting that the spin–spin correlations in the transverse direction have a very short range, the difference between the extrapolated values of $J_\mathrm{d} = 0$ and $J_\mathrm{d} = J_\mathrm{d}^{\max}$ appears to be relatively large. We believe that this difference could be inferred from the fact that the extrapolations from 2D systems were done with lattice sizes up to $L = 12$ only.

3.5. Spin–spin correlations on large systems

So far, in the study of $S = 1$ systems, we have fixed $J_\perp = 0.4$. This choice was motivated by the presence of $\Delta_\mathrm{H} = 0.4107$ in an isolated chain. We initially felt that it was necessary to choose a large enough $J_\perp$ that the chains will effectively be coupled when the perturbation is turned on and this will lead to sizable correlation in the thermodynamic limit. But this choice limited us to relatively small lattices, $L \lesssim 12$. This is because when $J_\perp$ is large, the condition $\delta E/J_\perp \gg 1$ is hard to fulfil for larger L. For instance for $L = 16$, $\delta E/J_\perp = 5.65$ for $m_2 = 64$, this prevented us from studying $L = 16$ lattices. But in the course of this work, we find that even smaller values of $J_\perp$ can lead to detectable values in the unfrustrated regime C_l as $l \to \infty$. For smaller $J_\perp$, we can actually reach larger L. We wish to present in this part our results for $J_\perp = 0.2$ and $L = 24$. These results will add strength to those for $J_\perp = 0.4$ presented above.

In figure 15, we show the longitudinal correlation,

$$\bar{C}_l = \langle S_{L/2+1,L/2+1} S_{L/2+l,L/2+1} \rangle, \tag{13}$$

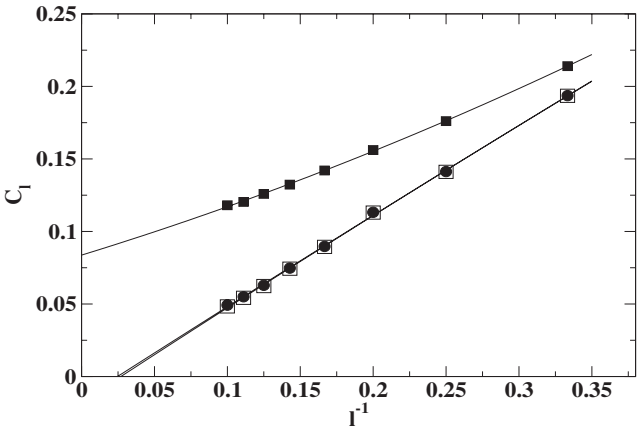

Figure 15. Longitudinal spin–spin correlation as a function of the distance for $L = 24$, $S = 1$, $J_\perp = 0$, $J_\mathrm{d} = 0$ (filled circles), $J_\perp = 0.2$, $J_\mathrm{d} = 0$ (filled squares) and $J_\perp = 0.2$, $J_\mathrm{d} = 0.102$ (open squares).

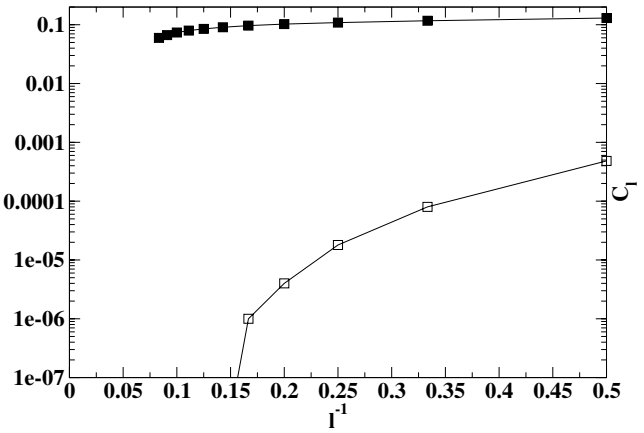

Figure 16. Transverse spin–spin correlation as a function of the distance for $L = 24$, $S = 1$, $J_\perp = 0.2$, $J_\mathrm{d} = 0$ (filled squares) and $J_\mathrm{d} = 0.2$, $J_\mathrm{d} = 0.102$ (open squares).

taken in the middle chain. For $J_\perp = 0.2$ and $J_\mathrm{d} = 0$, $\bar{C}_l$ clearly extrapolates to a finite value as expected. But for $J_\perp = 0.2$ and $J_\mathrm{d} = 0.102$, $\bar{C}_l$ is nearly identical to the spin–spin correlation on an isolated chain. For the transverse correlation C_l shown in figure 16, we see again the dramatic difference between the unfrustrated and highly frustrated cases. In the first case, C_l goes to a finite value when $l \to \infty$, but for the highly frustrated case, C_l decays exponentially.

Another picture of this dramatic difference is given by the magnetic structure factor $S(K = (k_x, k_y))$ shown in figures 17 and 18. In the magnetic phase, $S(K)$ is dominated by a sharp peak at $K = (\pi, \pi)$ indicative of Néel order. In the disordered phase, $S(K)$ is nearly flat except for a small range along $K = (\pi, k_y)$ which retains the signature of short range intra-chain correlations.

J. Stat. Mech. (2006) P02002

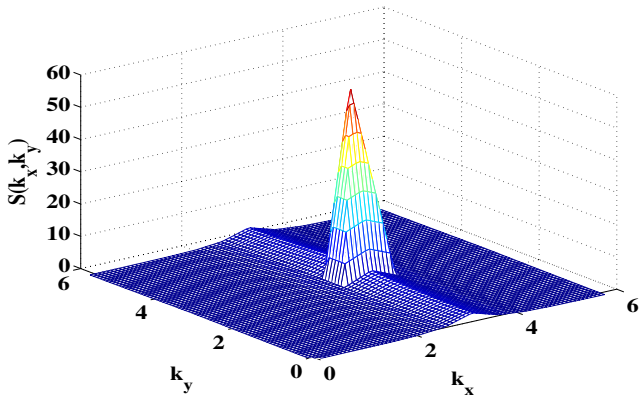

Figure 17. Magnetic structure factor for $L = 24$, $S = 1$, $J_\perp = 0.2$, $J_\mathrm{d} = 0$.

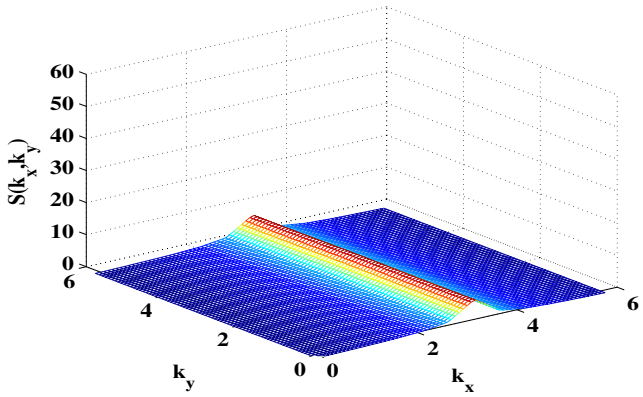

Figure 18. Magnetic structure factor for $L = 24$, $S = 1$, $J_\perp = 0.2$, $J_\mathrm{d} = 0.102$.

3.6. Conclusion

In this section, we have presented comprehensive results on $S = 1$ coupled chains. These results show some analogy with those for $S = \frac{1}{2}$ published in [22]. Starting from the unfrustrated system for which $J_\mathrm{d} = 0$, the ground state for $S = 1$ is ordered, as expected from the DLS theorem. While for $S = \frac{1}{2}$ it was necessary to simulate lattices of up to $L = 64$ [25] in order to see the extrapolation of C_l to a finite value, for $S = 1$ relatively small sizes ($L = 12$) were enough. This is because quantum fluctuations are less important in a $S = 1$ system, i.e., the order parameter is larger. This enables it to be computed more easily. By comparison, the same extrapolation done for $S = \frac{1}{2}$ will lead to a negative value.

When the frustration J_d is turned on and reaches the value $J_\mathrm{d}^{\max}$, a point where E_G is maximum, C_l decays exponentially, Δ takes a value very close to that of a pure 1D system. These results imply that at $J_\mathrm{d}^{\max}$, the transverse interactions are irrelevant. For $S = \frac{1}{2}$, we identified this state as a spin version of an SLL. In that case, this sliding phase will probably be confined at the critical point where the two competing magnetic states $K = (\pi, \pi)$ and $K = (\pi, 0)$ neutralize each other. However, we cannot completely rule out a small finite extension of the sliding phase or even totally exclude the emergence of a relevant interaction at lower energies which eventually drives the system to a dimerized

J. Stat. Mech. (2006) P02002

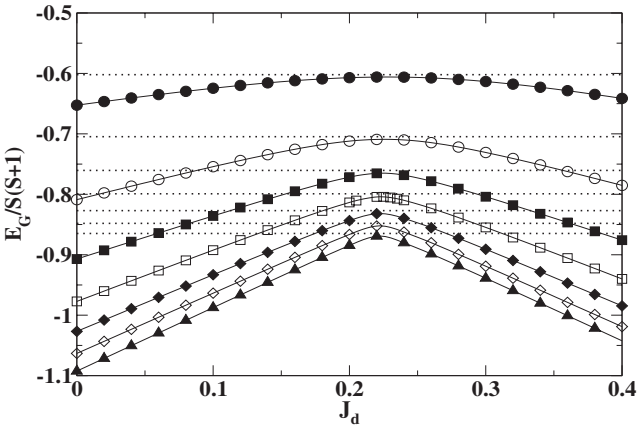

Figure 19. Ground state energy as a function of J_d and $S = \frac{1}{2}$ (filled circles), $S = 1$ (open circles), $S = \frac{3}{2}$ (filled squares), $S = 2$ (open squares), $S = \frac{5}{2}$ (filled diamonds), $S = 3$ (open diamonds), $S = \frac{7}{2}$, (filled triangles).

phase [13]. It is obvious that, though both $S = \frac{1}{2}$ and 1 systems are made of nearly disconnected chains at $J_\mathrm{d}^\mathrm{max}$, the conclusions must be different because of the presence of the Haldane gap Δ_H in the $S = 1$ chain. The existence of Δ_H restricts the possible phases that may arise in the vicinity of $J_\mathrm{d}^\mathrm{max}$. The first crucial difference is that the disordered state that exists in an $S = 1$ system has a gap in its excitation spectrum as seen in figure 14; any eventual residual interaction will be wiped out by this gap which means that the emergence of new phases at low energies is not favourable for an $S = 1$ system. This disordered phase probably has a finite extension which is roughly $\propto\Delta_\mathrm{H}$.

4. Results for $S = \frac{1}{2}$ to 4

In the study of various S, we will not do the same extensive calculation as was seen in the preceding section with $S = 1$. We will simply fix L and analyse the behaviour of the system as a function of J_d and l. As we will see below, quantum fluctuations are small for $S > 1$; the study of relatively small systems is enough to get the correct picture in the thermodynamic limit. We studied a lattice with $L \times (L + 1) = 10 \times 11$ for $S = \frac{1}{2}$ to 4. $J_\perp$ was set to 0.4 so that it is larger than the finite size gap in half-integer spin systems and larger than or close to the Haldane gaps in integer spin systems. J_d is varied from 0 to 0.4.

4.1. Ground state energies

The ground state energy is shown in figure 19 for $S = \frac{1}{2}$ to $\frac{7}{2}$. Simulations were also done for $S = 4$ but they did not converge for certain values of J_d. We impute this failure to the large degeneracy of the renormalized single-chain Hamiltonian h_l for large S. At $J_\mathrm{d} = 0$, the curves approach the classical value $E_\mathrm{G}/S^2 = -1.4$ quite rapidly. For $S = \frac{7}{2}$, we find $E_\mathrm{G}/S(S = 1) = -1.093$. But if we use the $1/S^2$ normalization, we get $E_\mathrm{G}/S^2 = -1.405$. Hence if both finite size effects and the correct normalization are taken into account, $S = \frac{7}{2}$ is already in the classical limit.

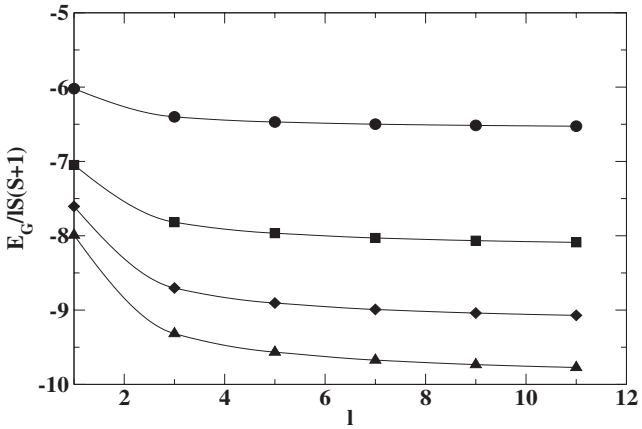

Figure 20. Ground state energy at $J_\mathrm{d} = 0$ as a function of l and $S = \frac{1}{2}$ (circles), $S = 1$ (squares), $S = \frac{3}{2}$ (diamonds), $S = 2$ (triangles).

Larger spin systems are found to present the same features as are displayed by spin 1/2 systems. The ground state energy, E_G, shown in figure 19 increases as J_d increases until the maximally frustrated point where E_G of the two-dimensional system becomes very close to that of disconnected chains. From this point it decreases when J_d is further increased. This may be interpreted as follows: starting from the Néel state with $K = (\pi, \pi)$ for $J_\mathrm{d} = 0$, the system tends to lose energy under the action of J_d which progressively destroys the Néel order until the maximally frustrated point is reached. Beyond this point, J_d becomes dominant and the systems enters the Néel $K = (\pi, 0)$ phase. The position of this maximum decreases slowly with increasing S. This indicates that in addition to the effect of OBC that shifts $J_\mathrm{d}^{\max}$ towards higher values, there are intrinsic finite size effects. All systems evolve regularly towards the $S \to \infty$ limit.

The curve of E_G appears to change structure as S increases. At low S, a well rounded maximum is observed. We were able to fit all the points of the curve to a quadratic function. But for large S, this became impossible. The maximum has nearly become a cusp as for $S \to \infty$. This cusp is at the intersection of two straight lines $E_{\mathrm{G}_1} = -1 - J_\perp + 2J_\mathrm{d}$ and $E_{\mathrm{G}_2} = -1 + J_\perp - 2J_\mathrm{d}$ which are the ground state energies, respectively, below and above the transition point $J_\mathrm{d} = 0.5J_\perp$.

$E_\mathrm{G}(l)$ shown in figures 20, 21 displays the features seen for $S = 1$. It decreases when l increases in the weak frustration regime. It remains nearly constant in the vicinity of the maximally frustrated point.

4.2. First-neighbour correlation

The tendency towards severing of the chains is more clearly seen in the transverse bond strength

$$C_1 = \langle S^z_{5,6} S^z_{5,7} \rangle, \tag{14}$$

shown in figure 22. In all cases, C_1 decreases from its value at $J_\mathrm{d} = 0$ and seems to vanish at J_d^0 (we were able in all cases to reach values of C_1 which are equal to or less than the numerical accuracy of our simulations). From this point it increases. There is a

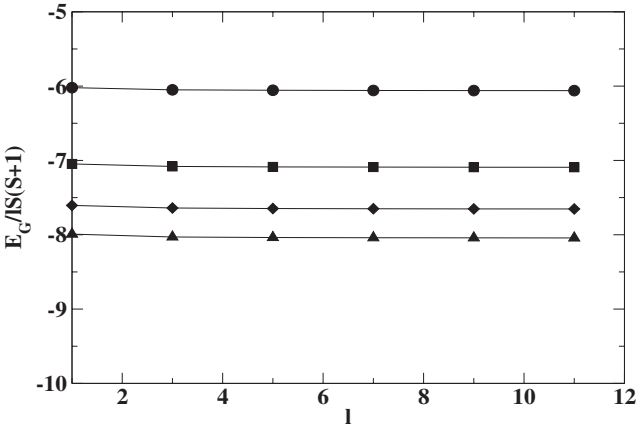

Figure 21. Ground state energy at $J_\mathrm{d} = 0$ as a function of l and $S = \frac{1}{2}$ (circles), $S = 1$ (squares), $S = \frac{3}{2}$ (diamonds), $S = 2$ (triangles).

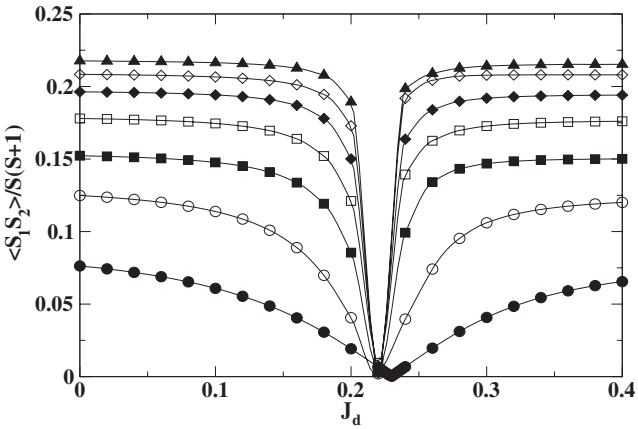

Figure 22. First-neighbour correlation as a function of J_d and $S = \frac{1}{2}$ (circles), $S = 1$ (squares), $S = \frac{3}{2}$ (diamonds), $S = 2$ (triangles) $S = \frac{5}{2}$ (filled diamonds), $S = 3$ (open diamonds), $S = \frac{7}{2}$, (filled triangles).

small difference between the position of J_d^0 for different values of S as found for E_G. The curves of C_1 suggest that for all S, the mechanism for avoiding frustration is identical: the systems relax to nearly disconnected chains. These curves also show the influence of quantum fluctuations for small S. This is seen in the decay of C_1 as soon as $J_\mathrm{d} \neq 0$. For larger S, C_1 remains nearly constant until $J_\mathrm{d} \approx J_\mathrm{d}^0$.

4.3. Long distance correlations

Since our starting point for 2D systems is disconnected chains, it is important to show, as for the spin 1/2 case studied previously, that the TSDMRG is able to reach the ordered phase. One possible way to look at the appearance of the ordered state is to look at the decay of the transverse correlation function,

$$C_l = \langle S^z_{5,6} S^z_{5,5+l} \rangle, \tag{15}$$

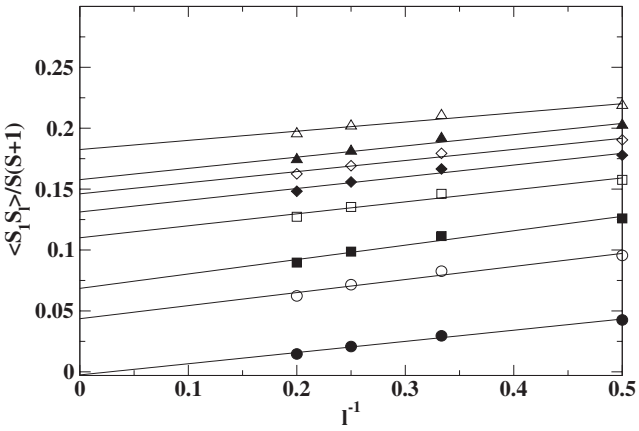

Figure 23. Spin–spin correlation at $J_\mathrm{d} = 0$ as a function of l and $S = \frac{1}{2}$ (filled circles), $S = 1$ (open circles), $S = \frac{3}{2}$ (filled squares), $S = 2$ (open squares), $S = \frac{5}{2}$ (filled diamonds), $S = 3$ (open diamonds), $S = \frac{7}{2}$, (filled triangles), $S = 4$ (open triangles).

in the Néel phase for $J_\mathrm{d} = 0$. We found that for all values of S except $S = \frac{1}{2}$, as shown in figure 23, the transverse correlation function extrapolates to finite values. C_l extrapolates to a negative value for $S = \frac{1}{2}$. In that case, quantum fluctuations are so strong that it is necessary to go to larger values of L as was done in [25].

At the maximally frustrated point, we also observe exponential decay of C_l similar to that for $S = \frac{1}{2}$. As seen in figure 24, this decay becomes less fast with increasing S. Indeed in the limit $S \to \infty$, the transition is of first order. The chains are disconnected in this classical limit and C_l is exactly equal to zero. However, for any small deviation from the transition point, the system falls into one of the ordered states. This point is virtually impossible to find exactly numerically. However, for smaller values of S the critical region is larger and even if we miss the exact transition point, this behaviour will nevertheless be observed as long as we are close enough to the QCP.

4.4. Spin gaps

The curves of $\Delta(J_\mathrm{d})$ in figure 25 for different values of S typically have a peak at $J_\mathrm{d} = J_\mathrm{d}^{\max}$. This peak is very narrow, except for $S = \frac{1}{2}$ where quantum fluctuation effects lead to a broader peak. As expected from the behaviour of C_1, this peak becomes sharper with increasing S. $\Delta(J_\mathrm{d}^{\max})$ is nearly equal to the finite size gap of an isolated chain which is represented by a flat line in each case. We were unable to reach the 1D gap for $S > \frac{3}{2}$. This is probably due to the narrowness of the critical region which makes it difficult to see the nearly disconnected chain regime. One can easily fall into one of the ordered regimes, leading to a relative slow decay of C_l which manifests itself in a smaller finite size gap.

4.5. Conclusion

In this section, we presented results for $L = 10$ and $J_\perp = 0.4$ with S varying from $\frac{1}{2}$ to 4. In agreement with the DLS theorem, we found long range order for all S greater than or equal to 1 in the unfrustrated case. As J_d is turned on, the long range order is destroyed.

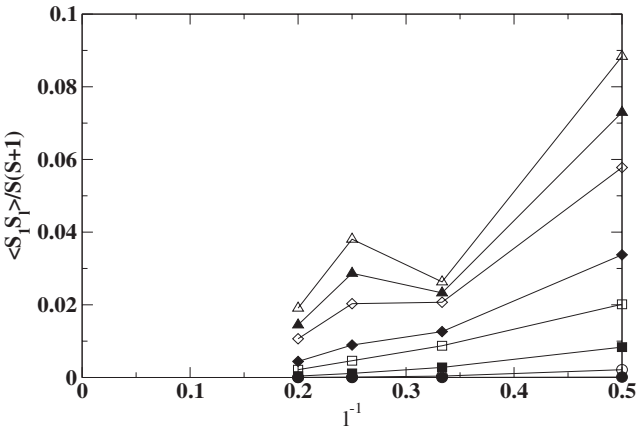

Figure 24. Transverse spin–spin correlation at $J_\mathrm{d} = 0.22$ as a function of l and $S = \frac{1}{2}$ (circles), $S = 1$ (squares), $S = \frac{3}{2}$ (diamonds), $S = 2$ (triangles), $S = \frac{5}{2}$ (filled diamonds), $S = 3$ (open diamonds), $S = \frac{7}{2}$, (filled triangles), $S = 4$ (open triangles).

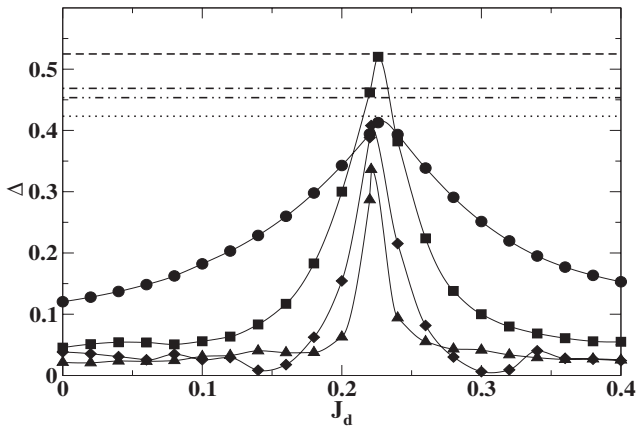

Figure 25. Spin gap as a function of J_d and $S = \frac{1}{2}$ (circles), $S = 1$ (squares), $S = \frac{3}{2}$ (diamonds), $S = 2$ (triangles).

An interesting question is that of the nature of this disordered state as a function of S. Before addressing this question, we will first review how frustration works in 1D [38].

For the frustrated $S = \frac{1}{2}$ chain, there is a transition to a dimerized phase at $J_{2\mathrm{c}} = 0.242J_1$, where $J_{2\mathrm{c}}$ is the value of next nearest neighbour coupling at the critical point. At this point a gap opens exponentially and grows with J_2. At $J_2 = 0.5J_1$, the system is perfectly dimerized and shows incommensurate correlation above this point (disordered point). At about $J_2 = 0.52J_1$ a two-peak structure appears in the structure factor (the Lifshitz point). DMRG simulations for the $S = \frac{3}{2}$ chain show a similar behaviour. This suggests that it is generic to half-integer spin systems.

Integer spin chains are already gapped in the absence of the frustration term J_2. For $S = 1$, the transition to a dimerized phase is absent, but numerical simulations show the presence of the disordered and the Lifshitz points. In addition there is a first-order transition at $J_2 = 0.75J_1$ from a phase with a single-string order to a phase with a double-

string order. At this point the chain splits into two chains. These special points are also observed in the $S = 2$ chain except that the order parameter for the first-order transition is still unknown.

The results presented in the preceding sections show that the mechanism for easing frustration works differently in 2D systems. This mechanism is the same for all values of S. The system spontaneously severs the frustrated bond at the maximally frustrated point. The similarity for all S of these mechanisms stems from the fact that if the transverse coupling is large enough, all the 2D systems are ordered for half-integer as well as for odd integer systems. Frustration is a competition between two magnetic ground phases and we have shown that for coupled chain systems, the best way to avoid frustration is to relax into nearly independent chains. It is clear that such a mechanism will be independent of the value of the spin as found in our numerical study. The consequences are nevertheless different for half-odd-integer and for integer spin systems.

For all half-odd-integer spin systems, like for the spin 1/2 studied more extensively in [22], there is a second-order phase transition between the two magnetic states at $J_\mathrm{d} = J_\mathrm{d}^{\max}$. At the critical point, the system is disordered. The transverse correlation decays exponentially while, at long distances, the longitudinal one behaves like those of independent chains. Hence at the critical point, the spin rotational symmetry of the Hamiltonian is restored. As for spin 1/2, there might be a residual interaction which can drive the system eventually to a SP phase. But previous numerical studies on 2D systems [22] and on three-leg ladders point to the absence of a dimerized phase in this region for $S = \frac{1}{2}$. This is expected to be valid for all half-odd S. We would like to stress that dimerization is not the driving mechanism in the formation of the disordered state. We are indeed aware of earlier ED results [31] in which an enhancement of the SP susceptibility was observed in the regime $J_2 \approx J_1/2$. We believe in light of our results that this is merely the consequence of the severing of the chains in one of the two directions of the square lattice. The SP signal is expected to be larger in 1D where it has a power law decay than in 2D when the spins are locked into Néel order in the unfrustrated regime.

For integer spins, there is an intermediate phase between the two magnetic states. When $|J_\perp - 2J_\mathrm{d}| \ll \Delta$, where Δ is the single-chain spin gap, the transverse couplings are irrelevant. The maximally frustrated point is the equivalent of the disordered point seen in 1D. In this regime of couplings, the system is an assembly of nearly decoupled chains. In the case of integer spins, even if there is a residual interaction at the maximally frustrated point, this interaction is necessary irrelevant because of the presence of Δ. Integer spin systems are thus radically different from half-odd-integer systems.

5. Conclusion

In this paper, we used the TSDMRG to study coupled spin chains with S varying from $\frac{1}{2}$ to 4. This study illustrates the power of the TSDMRG method, where using a modest computer effort we were able to study the unfrustrated regime and find long range magnetic order, in agreement with the DLS theorem and Monte Carlo studies. We obtained good accuracy in the highly frustrated regime of the model. The study of this region has so far resisted other numerical methods.

We showed that in order to avoid frustration, all spin systems tend to sever the frustrated bonds. The severing of the transverse bonds is a large effect which is seen in

doi:10.1088/1742-5468/2006/02/P02002

various physical quantities. The strong frustration regime is dominated by 1D physics; topological effects become important as predicted in [7, 8, 21]. However, we did not find any qualitative difference between odd and even integer spin systems as predicted in [7, 21]. This could be due to the fact that in the highly frustrated regime the 2D systems tend to relax into nearly independent 1D systems where topological effects are identical for odd and even integer spins. It could also be related to the anisotropy of the model studied.

Acknowledgments

The author wishes to thank K L Graham for reading the manuscript. This work was supported by the NSF Grant No DMR-0426775.

References

[1] Dyson F J, Lieb E H and Simon B, 1978 *J. Stat. Phys.* **18** 335
[2] Neves E J and Peres J F, 1986 *Phys. Lett.* A **114** 331
[3] Reger J D and Young A P, 1988 *Phys. Rev.* B **37** 5978
[4] Dombre T and Read N, 1988 *Phys. Rev.* B **38** 7181
[5] Fradkin E and Stone M, 1988 *Phys. Rev.* B **38** 7215
[6] Wen X-G and Zee A, 1988 *Phys. Rev. Lett.* **61** 1025
[7] Haldane F D M, 1988 *Phys. Rev. Lett.* **61** 1029
[8] Affleck I, 1988 *Phys. Rev.* B **37** 5186
[9] Vishwanath A and Carpentier D, 2001 *Phys. Rev. Lett.* **86** 676
[10] Emery V J, Fradkin E, Kivelson S A and Lubensky T C, 2000 *Phys. Rev. Lett.* **85** 2160
[11] Mukhopadhyay R, Kane C L and Lubensky T C, 2001 *Phys. Rev.* B **64** 045120
[12] Nersesyan A A and Tsvelik A M, 2003 *Phys. Rev.* B **67** 024422
Tsvelik A M, 2004 *Phys. Rev.* B **70** 134412
[13] Starykh O A and Balents L, 2004 *Phys. Rev. Lett.* **93** 127202
[14] Hager G, Jeckelmann E, Feske H and Wellein G, 2004 *J. Comput. Phys.* **194** 795
[15] Moukouri S and Alvarez J V, 2005 *Phys. Lett.* A **344** 387
[16] White S R, 1992 *Phys. Rev. Lett.* **69** 2863
White S R, 1993 *Phys. Rev.* B **48** 10345
[17] Misguich G and Lhuillier C, 2004 *Frustrated Spin Systems* ed H T Diep (Singapore: World Scientific)
[18] Sindzingre A, 2004 *Phys. Rev.* B **69** 094418
[19] Haldane F D M, 1983 *Phys. Lett.* A **93** 464
Haldane F D M, 1983 *Phys. Rev. Lett.* **50** 1153
[20] Lieb E, Schultz T and Mattis D, 1961 *Ann. Phys., NY* **16** 407
[21] Read N and Sachdev S, 1991 *Phys. Rev. Lett.* **66** 1773
[22] Moukouri S, 2005 *Preprint* cond-mat/0504306 (unpublished)
[23] Fradkin E, 1991 *Field Theories of Condensed Matter Systems* ed D Pines (Boulder, CO: West View Press)
[24] Moukouri S and Caron L G, 2003 *Phys. Rev.* B **67** 092405
[25] Moukouri S, 2004 *Phys. Rev.* B **70** 014403
[26] Moukouri S, 2005 *Preprint* cond-mat/0510288
[27] Alvarez J V and Moukouri S, 2005 *Int. J. Mod. Phys.* C **16** 843
[28] Wilson K G, 1975 *Rev. Mod. Phys.* **47** 773
[29] Wang X, Zhu N and Chen C, 2002 *Phys. Rev.* B **66** 172405
[30] Affleck I and Qin S, 1999 *J. Phys. A: Math. Gen.* **32** 7815
[31] Dagotto E and Moreo A, 1989 *Phys. Rev. Lett.* **63** 2148
[32] Affleck I and Marston J B, 1988 *Phys. Rev.* B **37** 3774
[33] Affleck I, Kennedy T, Lieb E H and Tasaka H, 1988 *Commun. Math. Phys.* **115** 477
[34] Wen X-G, Wilczeck F and Zee A, 1989 *Phys. Rev.* **39** 11413
[35] Kotliar G, 1988 *Phys. Rev.* B **37** 3664
[36] Baskaran G, Zou Z and Anderson P W, 1987 *Solid State Commun.* **63** 973
[37] Senthil T, Vishwanath A, Balents L, Sachdev S and Fisher M P A, 2004 *Science* **303** 1490
[38] Roth R and Schollwöck U, 1998 *Phys. Rev.* **58** 9264

J. Stat. Mech. (2006) P02002